UC Irvine

UC Irvine Previously Published Works

Title

A constitutive framework for predicting weakening and reduced buttressing of ice shelves based on observations of the progressive deterioration of the remnant Larsen B Ice Shelf

Permalink

https://escholarship.org/uc/item/4695s1s2

Journal

Geophysical Research Letters, 43(5)

ISSN

0094-8276

Authors

Borstad, Chris
Khazendar, Ala
Scheuchl, Bernd
et al.

Publication Date

2016-03-16

DOI

10.1002/2015gl067365

Peer reviewed

eScholarship.org Powered by the California Digital Library
University of California

AGU PUBLICATIONS

Geophysical Research Letters

RESEARCH LETTER
10.1002/2015GL067365

Key Points:
- Assimilated observations indicate progressive weakening of ice shelf from 2000 to 2015
- New framework introduced for viscous ice deformation with analytical solution for damage
- New framework reproduces observed weakening and is generalizable to any ice shelf

Supporting Information:
- Supporting Information S1

Correspondence to:
C. Borstad,
chris.borstad@unis.no

Citation:
Borstad, C., A. Khazendar, B. Scheuchl, M. Morlighem, E. Larour, and E. Rignot (2016), A constitutive framework for predicting weakening and reduced buttressing of ice shelves based on observations of the progressive deterioration of the remnant Larsen B Ice Shelf, *Geophys. Res. Lett.*, *43*, 2027–2035, doi:10.1002/2015GL067365.

Received 9 DEC 2015
Accepted 9 FEB 2016
Accepted article online 11 FEB 2016
Published online 4 MAR 2016

©2016. American Geophysical Union. All Rights Reserved.

A constitutive framework for predicting weakening and reduced buttressing of ice shelves based on observations of the progressive deterioration of the remnant Larsen B Ice Shelf

Chris Borstad[1], Ala Khazendar[2], Bernd Scheuchl[3], Mathieu Morlighem[3], Eric Larour[2], and Eric Rignot[2,3]

[1]Department of Arctic Geophysics, University Centre in Svalbard, Longyearbyen, Norway, [2]Jet Propulsion Laboratory, California Institute of Technology, Pasadena, California, USA, [3]Department of Earth System Science, University of California, Irvine, California, USA

Abstract The increasing contribution of the Antarctic Ice Sheet to sea level rise is linked to reductions in ice shelf buttressing, driven in large part by basal melting of ice shelves. These ocean-driven buttressing losses are being compounded as ice shelves weaken and fracture. To date, model projections of ice sheet evolution have not accounted for weakening ice shelves. Here we present the first constitutive framework for ice deformation that explicitly includes mechanical weakening, based on observations of the progressive degradation of the remnant Larsen B Ice Shelf from 2000 to 2015. We implement this framework in an ice sheet model and are able to reproduce most of the observed weakening of the ice shelf. In addition to predicting ice shelf weakening and reduced buttressing, this new framework opens the door for improved understanding and predictions of iceberg calving, meltwater routing and hydrofracture, and ice shelf collapse.

1. Introduction

Many of the largest and fastest changes to the Antarctic ice sheet over the last decade have been linked to the thinning and loss of ice shelves in a manner that is consistent, at least qualitatively, with notions of ice shelf buttressing [*Intergovernmental Panel on Climate Change*, 2013]. To predict the fate of the ice sheet, therefore, the dominant physical mechanisms of ice shelf evolution must be accurately represented in models. Ocean-driven basal melting of ice shelves [*Pritchard et al.*, 2012; *Rignot et al.*, 2013] is believed to be the predominant cause of ice shelf buttressing losses. However, as ice shelves thin they also become more susceptible to fracture [*Shepherd et al.*, 2003]. In West Antarctica, fracturing and weakening of ice shelf shear margins appears to be compounding the buttressing losses associated with ice shelf thinning [*MacGregor et al.*, 2012]. The irreversible collapse of the West Antarctic Ice Sheet, which is speculated to already be underway [*Rignot et al.*, 2014; *Joughin et al.*, 2014], may have been hastened by the combined effects of thinning and mechanical weakening of buttressing ice shelves. Yet the mechanisms of fracture-induced weakening are poorly understood and still absent in projections of ice shelf evolution. Although advances in ice-ocean model coupling [*Goldberg et al.*, 2012; *Hellmer et al.*, 2012] are providing insight into feedbacks driven by warming oceans, ice sheet models are still failing to capture associated changes in bulk ice rheology and buttressing due to mechanical weakening of ice shelves.

To address this need, we first assemble the longest available time series to date of ice shelf weakening. We then devise a new constitutive formalism that is consistent with the observations and generalizable to represent other glaciological processes involving fractures. We focus here on the remnant Larsen B Ice Shelf (RLBIS, Figure 1a), the surviving portion of the ice shelf that filled the Larsen B embayment prior to its partial collapse in 2002. The buttressing provided by RLBIS diminished over the period 2000 to 2010 [*Khazendar et al.*, 2015], which has facilitated the thinning and acceleration of its tributary glaciers [*Scambos et al.*, 2014; *Khazendar et al.*, 2015].

Using remote sensing observations assimilated in the Ice Sheet System Model (ISSM) [*Larour et al.*, 2012], we calculate the spatial pattern of ice damage for the years 2000, 2006, 2010, and 2015 (Figure 1). We then analyze

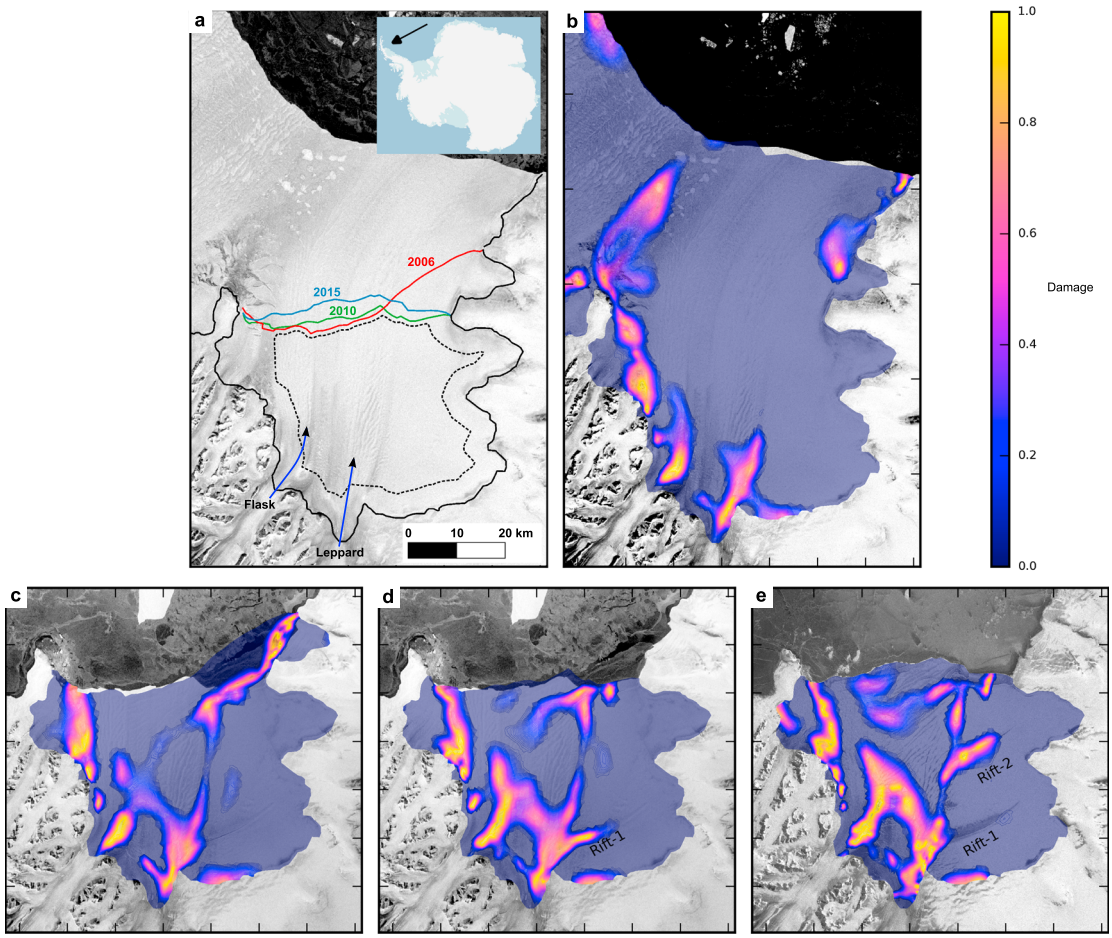

Figure 1. Evolution of damage for the Larsen B Ice Shelf from assimilated observations. (a) The ice shelf in a RADARSAT-1 backscatter amplitude mosaic from 2000. Ice front position in later years indicated by labeled lines. Solid black line indicates boundary between floating and grounded ice; dotted line encloses region used for analysis of damage evolution. Arrows indicate location and flow direction of Flask and Leppard tributary glaciers. (b) Damage in 2000, overlaid on the same 2000 RADARSAT-1 mosaic. (c) Damage in 2006, overlaid on a 2008 RADARSAT-2 backscatter amplitude mosaic. (d) Damage in 2010, overlaid on the same 2008 RADARSAT-2 mosaic. (e) Damage in 2015, overlaid on an April 2015 Sentinel-1a backscatter image.

the constitutive parameter space defined through time by the weakening ice shelf. Based on the characteristic shape of the parameter space, we devise a generalization of the constitutive relationship for viscous ice deformation that explicitly defines damage once a threshold stress is reached in the ice. We implement this new framework in the ice sheet model and are able to reproduce most of the observed weakening of the ice shelf through time, especially in the shear margins where buttressing stresses are highest. We conclude with an outlook on how this new framework can be generalized to other ice shelves and used to study and model other glaciological processes involving fractures.

2. Inverse Damage Calculation

We begin by quantifying ice shelf damage from remote sensing observations. Damage in this context is a state variable that represents fracture-induced enhancement of viscous ice deformation [*Borstad et al.*, 2013]. Damage is taken here as a scalar variable that takes values between zero, for fully intact ice, to one for ice that has lost all load bearing capacity. The inverse damage calculation [*Borstad et al.*, 2013] involves first determining the spatial rheology of the ice shelf using a control method [*Larour et al.*, 2005] that seeks a spatial pattern of the ice viscosity parameter B (equation (2)) that minimizes the misfit between observed and modeled surface velocity data. We implement the algorithm in an ice sheet model [*Larour et al.*, 2012] that utilizes the finite element method. We use a cost function that measures the $\mathcal{L}^2$ misfit between modeled and observed horizontal velocity components, and a Tikhonov regularization term that penalizes gradients in B. An unstructured triangular mesh with a spatial resolution varying from 300 to 1000 m is used to represent

the ice shelf. A depth-integrated approximation (Shallow Shelf Approximation) to the governing momentum balance equations is used [*MacAyeal*, 1989]. Horizontal surface velocities for the ice shelf are derived from satellite radar data, collected in 2000 by RADARSAT-1, in 2006 and 2010 by ALOS PALSAR, and in 2015 by Sentinel-1a, processed using speckle tracking [*Khazendar et al.*, 2015]. Ice shelf boundaries are drawn from grounding lines determined from differential satellite radar interferometry [*Rignot et al.*, 2011], and ice front positions are drawn manually from synthetic aperture radar (SAR) backscatter amplitude images for each year. Ice thickness and surface elevation from Bedmap2 are adopted [*Fretwell et al.*, 2013] and taken as representative for the year 2000. For 2006, 2010, and 2015, we update the shelf geometry by applying the observed average surface lowering trend of the shelf [*Fricker and Padman*, 2012], adjusting the thickness to maintain hydrostatic equilibrium of the ice.

To the best of our knowledge there are no in situ measurements of ice temperature for RLBIS. We thus carry out a range of inverse damage calculations based on different temperature assumptions that we believe bracket a reasonable expectation for the true ice temperature. In each case, we use the assumed temperature to specify the ice viscosity parameter $B = B(T)$ [*Cuffey and Paterson*, 2010] and provide an initial state $B_o = B(T)$ for the inversion algorithm. Damage is then calculated analytically [*Borstad et al.*, 2013] anywhere that the viscosity parameter determined from the inversion (B_i) is lower than would be expected for pure ice at the assumed temperature,

$$D = 1 - \frac{B_i}{B(T)}. \tag{1}$$

Equation (1) applies where $B_i < B(T)$, elsewhere $D = 0$. This calculation produces a spatial map of damage, from any source, that leads to enhanced flow. The source of damage could be a gradual viscous process or a short-timescale elastic process, as both can leave an imprint on the velocity field. Additional insight into ice shelf buttressing can be gleaned in areas where $B_i > B(T)$ [*Borstad et al.*, 2013; *Khazendar et al.*, 2015], though we focus only on damage here.

We consider four different temperature scenarios: a temperature distribution that varies horizontally based on a steady state balance of vertical advection and diffusion of heat in the ice column [*Holland and Jenkins*, 1999; *Borstad et al.*, 2012] and spatially uniform depth-averaged temperatures of −5°C, −7.5°C, and −10°C. Both the temperature and the ice viscosity parameter are considered as depth-averaged values here. It would be more physically realistic to first estimate a vertical temperature distribution $T = T(z)$ across the shelf and then parameterize the viscosity parameter $B = B(T(z))$ before integrating vertically. However, given the lack of observations of ice temperature for RLBIS (or for any other ice shelf, for that matter), the difference between $\overline{B(T(z))}$ and $B(\overline{T(z)})$ (where overbars indicate depth integration) is likely small compared to our assumed overall uncertainty in the true ice temperature.

We perform an *L* curve analysis [*Morlighem et al.*, 2013] to help determine an appropriate level of regularization for the inverse method, noting that we want to capture sharp gradients in flow caused by fractures while at the same time avoiding overfitting any artifacts in the data. To determine the sensitivity of our results to this somewhat subjective choice, we repeat the inverse damage calculation for the steady state temperature scenario with regularization turned off. The results presented here are from calculations using a uniform ice temperature of −7.5°C and using regularization in the inversion; analogous results for each of the remaining cases is presented in the supporting information (Figure S1).

3. Results and Discussion

3.1. Stress and Damage Evolution Through Time

We confirm earlier findings [*Borstad et al.*, 2012] that the shear margins of RLBIS were moderately weakened in 2000 when the full ice shelf still existed (Figure 1b). Since then, RLBIS has grown more damaged, both in the magnitude of damage in the shear margins and in the spatial extent of damage elsewhere (Figures 1c–1e). This progressive weakening explains the diminished buttressing provided by the shelf from 2000 to 2010 [*Khazendar et al.*, 2015].

The outstanding question is how to explain and model this evolution of damage through time. The standard constitutive relation ("flow law") for glacier ice [*Cuffey and Paterson*, 2010] can be generalized to account for a given level of damage [e.g., *Pralong and Funk*, 2005; *Borstad et al.*, 2013, 2012; *Krug et al.*, 2014; *Albrecht and Levermann*, 2014] as

$$\tau_e = (1 - D)\, B\, \dot{\varepsilon}_e^{1/n} \tag{2}$$

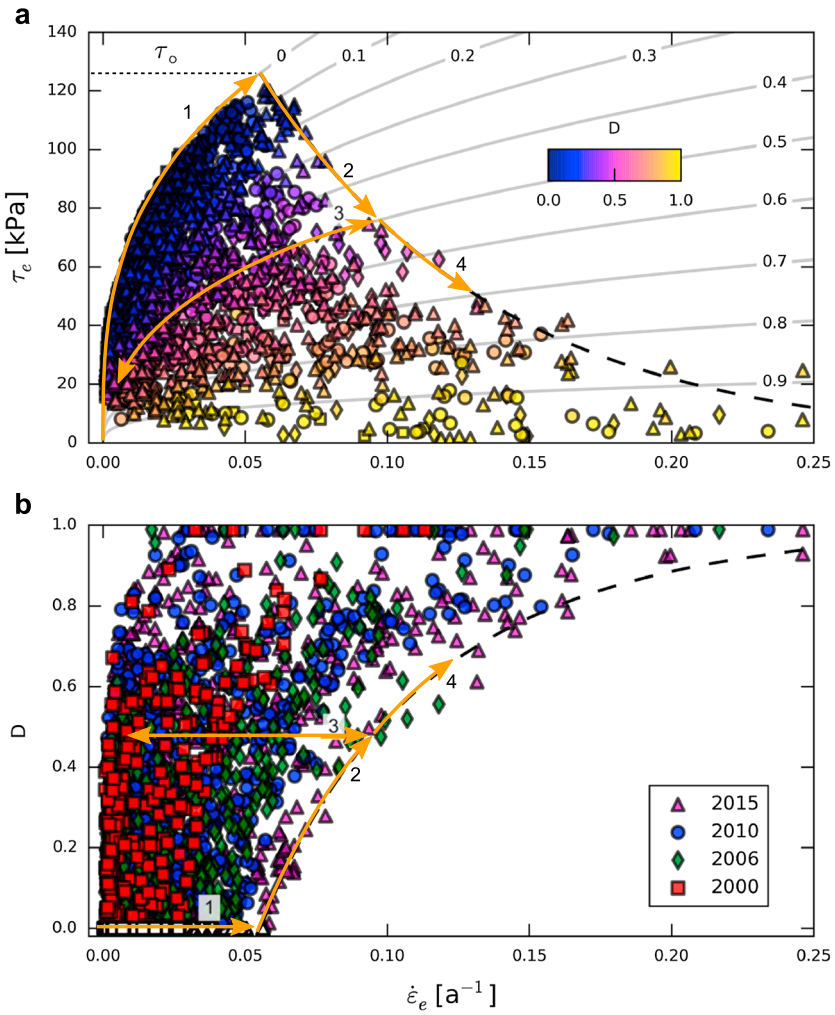

Figure 2. Constitutive parameter space defined by the ice shelf through time. (a) Effective deviatoric stress τ_e versus effective strain rate $\dot{\varepsilon}_e$ at nodes of the model mesh, with symbols colored by the inferred level of damage. Grey curves show the generalized flow law (equation (2)) at indicated levels of damage. Dashed curve indicates equation (3) for $\tau_o = 126$ kPa and $\kappa = 2.5$. (b) Damage D versus effective strain rate. Dashed curve indicates equation (4) for the same values of τ_o and κ. Orange curves in both panels indicate example scenario for stress and damage evolution according to the new constitutive framework, as described in text.

written here as a relationship between the scalar effective deviatoric stress $\left(\tau_e = \sqrt{1/2\tau_{ij}\tau_{ji}}\right)$ and scalar effective strain rate $\left(\dot{\varepsilon}_e = \sqrt{1/2\dot{\varepsilon}_{ij}\dot{\varepsilon}_{ji}}\right)$, where $0 \leq D < 1$ is the damage variable, B is the ice viscosity parameter (primarily dependent on temperature), and n is the power law exponent. For evolving the level of damage through time, a number of empirical source functions have been proposed to incrementally update damage as it advects with the flow. However, these parameterizations tend to be rather ad hoc [*Krug et al.*, 2014; *Albrecht and Levermann*, 2014] or tuned to small-scale laboratory data [*Pralong and Funk*, 2005; *Duddu and Waisman*, 2012] rather than large-scale deformation behavior. Furthermore, there is no physical basis for evolving a fracture-based variable as part of an advection scheme; fractures should be expected to evolve in response to the evolving balance of stresses in the ice.

We instead propose a scheme for addressing damage evolution within a generalized constitutive framework directly. To this end, we note that for a given ice temperature (and thus B) and a given value of n, the standard flow law (equation (2) for $D = 0$) is a single power law curve. However, the generalization of the flow law for arbitrary levels of damage leads to the perspective of a state *space* being defined by the ice shelf through time, rather than a single constitutive curve (Figure 2a). The parameter space for stress can be thought of as being composed of a family of flow law curves, each at a given level of damage (Figure 2a, grey curves).

Based on the shape of the stress space swept out through time as RLBIS deteriorates (Figure 2a, colored symbols), we propose a new framework for computing damage. First, although the flow law is commonly taken as applicable for any arbitrary level of stress, we observe that a clear threshold stress is apparent. Second, the maximum stress that can be supported at any given level of damage decreases with increasing damage; partially fractured ice cannot support stresses as high as unfractured ice. Both of these characteristics can be captured by defining a softening curve that envelops the parameter space and that is traversed once the threshold stress is reached. We propose an exponential relation for the effective stress that envelops the assimilated observations,

$$\tau_e = \tau_\circ \exp\left(-\frac{\dot{\varepsilon}_e - \dot{\varepsilon}_\circ}{\dot{\varepsilon}_\circ (\kappa - 1)}\right), \tag{3}$$

where $\tau_\circ$ is the threshold stress for damage initiation, $\dot{\varepsilon}_\circ$ is the strain rate at the threshold stress, and $\kappa > 1$ is a ductility parameter that defines the initial downward slope of the softening curve. Since the threshold strain rate ($\dot{\varepsilon}_\circ$) is uniquely defined by the flow law (equation (2)) at $D = 0$, only two new parameters ($\tau_\circ$ and κ) are needed to define the softening curve, both of which have clear physical interpretations.

3.2. Analytical Solution for Damage

An important consequence of this new approach is that damage can be calculated analytically as the stress balance evolves. By combining equations (2) and (3) and expressing the threshold stress ($\tau_\circ$) as a threshold strain rate ($\dot{\varepsilon}_\circ$) at $D = 0$, damage can be written as

$$D = 1 - \left(\frac{\dot{\varepsilon}_e}{\dot{\varepsilon}_\circ}\right)^{-1/n} \exp\left(-\frac{\dot{\varepsilon}_e - \dot{\varepsilon}_\circ}{\dot{\varepsilon}_\circ (\kappa - 1)}\right). \tag{4}$$

This relation defines damage at a given effective strain rate once the threshold strain rate is reached (Figure 2b) and only as long as the envelope stress defined by equation (3) is traced.

We illustrate an example load history scenario according to this new framework in Figure 2. As an initially undamaged volume of ice is loaded, it follows the standard flow law (Figure 2a, curve 1). The ice must begin to fracture (become damaged) once the threshold stress is reached, as should be expected physically. Anything causing a further increase in strain rate will cause the level of damage to increase, accompanied by a decrease in stress as the load bearing capacity is reduced (curve 2). If the strain rate is then relaxed the stress around crack tips will relax, so damage will cease to grow. We do not consider fracture healing or damage reduction here (equation (4) is thus not run in reverse with a reduction in strain rate, since damage healing should be expected to follow a different timescale and different processes than damage production). For any subsequent unloading and reloading, the generalized flow law (equation (2)) is followed at the new level of damage (curve 3) until the envelope curve is again reached. Any further increase in strain rate would result in further growth of damage and subsequent stress softening (curve 4) and so on. This loading-unloading example is based on observations and model formulations for strain softening and damage growth of laboratory-scale specimens of ice [*Sinha*, 1988], cohesive snow [*Borstad and McClung*, 2011], and other heterogeneous fracturing materials [*Bažant and Jirásek*, 2002]. Its adoption here is a recognition of the success of this type of formulation in analogous settings and materials.

3.3. Determination of New Constitutive Parameter Values

For determining $\tau_\circ$ and κ, we compare spatial areas of the ice shelf domain that overlap across all years. We ignore inversion results within 5 km of the grounding line (where the external thickness product is interpolated across the grounding line, and thus, the stress balance and inversion results are not reliable), within 1 km of the ice front (to avoid any artifacts in the velocity processing and due to uncertainty in determining the ice front position), and around any features of the ice shelf that cannot be confidently distinguished from sea ice or mélange in the imagery (as indicated in Figure 1a). Values of $\tau_\circ$ and κ are calibrated to align the curves represented by equations (3) and (4) against the data points in both stress and damage space (Figures 2 and S1 in supporting information).

We normalize for spatial differences in temperature when determining $\tau_\circ$ and κ. This is of course not necessary for the cases in which we assume a uniform ice temperature across the shelf. However, for consistency and generality, in each case we normalize the effective strain rate by the strain rate at the threshold stress, which depends on temperature through the viscosity parameter $B = B(T)$ in the flow law (equation (2)). For each of the cases considered (Figure 2 and supporting information Figure S1), both the stress and damage

parameter spaces can be effectively enveloped with the proposed exponential curves (equations (3) and (4), respectively). The values of the parameters $\tau_\circ$ and κ (supporting information Figure S1) are determined by manual adjustment in order to align the curves against the outer limits of the parameter space. This procedure is somewhat subjective, and slight variations in parameter values can produce curves that appear to align with the data nearly as well. However, the variability in parameter values associated with this procedure of fitting by visual inspection is smaller than the uncertainty associated with the unknown temperature of the ice.

From the assimilated observations for RLBIS over the period 2000–2015, we find $\tau_\circ = 130 \pm 14$ kPa and $\kappa = 2.8 \pm 0.4$. The predominant source of uncertainty is the unknown temperature of the ice, although the general shape of the parameter space, and thus the appropriateness of the softening curve, is robust with respect to this uncertainty (Figure S1 in the supporting information).

3.4. Evaluation of Framework in a Forward Model

As a validation test of this new constitutive framework, we model RLBIS forward in time from 2000 to 2015 with yearly time steps. We initialize the model with assimilated velocity and inferred damage from 2000 (Figure 1b). The model is forced at each time step with velocity and damage observations within a 5 km band downstream of the grounding line. Between years of available velocity observations and inverse damage solutions, we linearly interpolate the forcings. The ice thickness is reduced uniformly at a rate of 5 ma^{-1} in line with limited observations [*Fricker and Padman*, 2012; *Khazendar et al.*, 2015]. The ice thickness is updated and advected at each time step, with basal melting rates specified according to an ocean circulation model [*Borstad et al.*, 2012] and surface mass balance specified according to a regional atmospheric climate model [*van den Broeke and van Lipzig*, 2004]. In the absence of a scheme for evolving the ice shelf boundary through time, we choose the 2006 ice shelf outline for the forward model, since this outline represents a median ice front position for the later years in the simulation.

In the interior of the ice shelf, the velocity is calculated freely at each time step. After solving for the stress balance, the damage is updated (where appropriate) according to equation (4) with $\tau_\circ = 126$ kPa and $\kappa = 2.5$, values determined for the uniform −7.5°C temperature case that we also use here for the forward model. Damage is then advected to carry a history of previous weakening along with the flow. We do not consider damage healing, and we limit the maximum amount of damage at 0.9 to prevent the viscosity from going to zero and loss of numerical stability. We note that the results are somewhat sensitive to this choice of D_{max}, and future work is needed to determine an appropriate value (physically and numerically) for this term.

The forward model reproduces most of the observed weakening in 2006, 2010, and 2015 (Figures 3a–3c). The difference between the forward model and the observed damage (Figures 3d–3f) and between the modeled and observed velocity (Figures 3g–3i) grows through time, as to be expected for a prognostic model. In general, however, the prognostic model results agree quite well with the observations. The best agreement between the forward model and the observations is in the shear margins of the shelf. Shear margins are where an ice shelf generally bears the highest stresses [*Gudmundsson*, 2013]; therefore, the evolution of these regions is arguably the most important for ice shelf buttressing.

The most pronounced disagreement between the forward model damage and the inverse damage is in the central convergence zone of the Flask and Leppard tributary glaciers and around the two large rifts in the southern part of the shelf. Rifts are known to propagate in short, episodic bursts [*Bassis et al.*, 2005] over short timescales for which the ice responds predominantly elastically. There are signatures of these features in some of the velocity observations (large jumps in velocity across the rift flanks), which explain why they are partially represented as damaged in the observations (Figures 1d and 1e). In general, however, we would not expect a fully viscous model to produce features that are predominantly elastic such as rifts. It would be more appropriate physically to couple the viscous damage model with an elastic damage model [e.g., *Borstad and McClung*, 2011] to predict the initiation and propagation of these fractures.

The opening of Rift 1 and Rift 2 may explain the appearance of some of the inferred damage in the convergence zone of the Flask and Leppard tributary glaciers. This would especially be the case in the vicinity of Rift 1, which by early 2015 had flanks that were about 5 km apart near the Leppard shear margin. The opening of this rift would facilitate enhanced flow near the southern shear margin of the Flask flow unit, leading to a relative rotation of the flow in the Flask-Leppard convergence zone. This sort of "nonlocal" flow influence can cause problems when interpreting inversion results on an ice shelf, for which the stress balance is inherently nonlocal. For example, anomalously high inferred values of B have been reported upstream of a remote

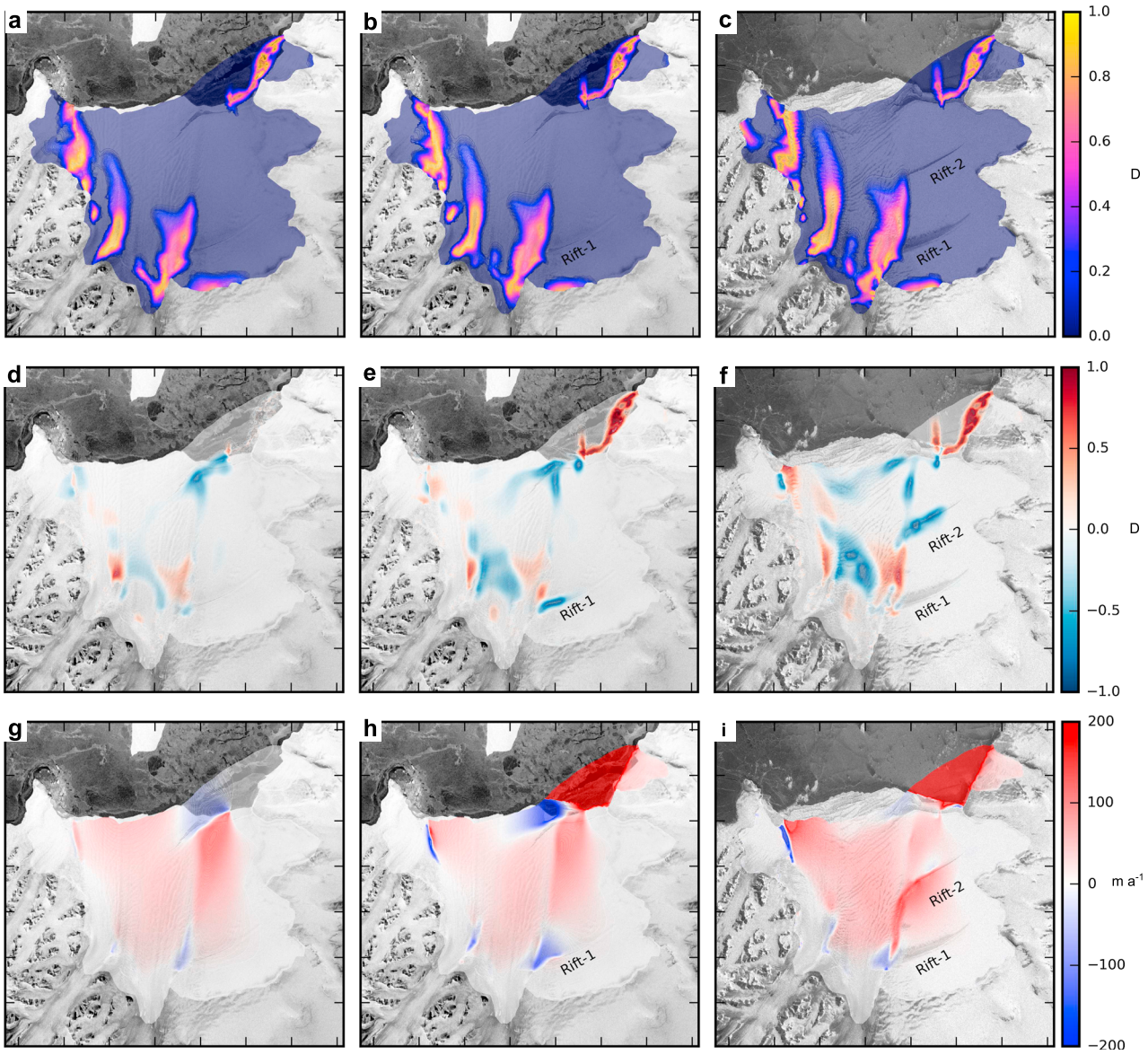

Figure 3. Prognostic damage calculations for the years (a) 2006, (b) 2010, and (c) 2015 for a model initialized with the inverse damage solution (Figure 1b) and velocity from 2000. (d–f) Modeled damage minus inverse damage for those respective years. (g–i) Modeled velocity minus observed (assimilated) velocity for those respective years. Results overlaid on the same radar images as in Figure 1.

pinning point (the Bawden Ice Rise) on the Larsen C Ice Shelf using similar inverse methods [*Khazendar et al.*, 2011; *Borstad et al.*, 2013]. The inversion algorithm in these studies produced very stiff ice in order to reproduce the observed, buttressed flow field. The Flask-Leppard convergence zone is likely to be the zone of strongest nonlocality of RLBIS since these are the two primary tributaries of the ice shelf. As these neighboring flow units converge and come into adjustment with each other, the local flow at any point is influenced by the push and pull of the neighboring flow unit. These nonlocal influences may complicate the interpretation of the inferred value of B, and thus damage, in this part of the ice shelf.

A further complication in interpreting the flow in the Flask-Leppard convergence zone relates to the ice temperature. This region of the ice shelf may be where the assumed temperature of the ice has the highest error. Basal accretion of marine ice, with resulting release of latent heat, has been predicted by an ocean circulation model applied to the cavity beneath this ice shelf [*Borstad et al.*, 2012]. The ice in this particular area of the shelf may be warmer, and thus softer, than we have assumed here. This would bias the damage calculation, creating artificial levels of damage to accommodate for the ice in the model being too cold.

Broadly speaking, most of the observed progressive weakening of RLBIS from 2000 to 2015 is consistent with gradual, viscous damage growth according to this new constitutive framework. This is especially encouraging given the simplicity of the model formulation. Fractures should, in general, be expected to induce some measure of anisotropy in a material. The fact that a scalar damage model, formulated using scalar measures of stress and strain rate, is able to reproduce most of the observed pattern of ice shelf weakening is promising. We expect that improvements can be made by formulating damage in tensor form and accounting for the full stress tensor. Healing of damage should also be accounted for and might be formulated by specifying a characteristic timescale for damage reduction under compressive stress states. A scheme for nonlocal regularization [e.g., *Borstad and McClung*, 2011] should also be implemented to prevent spurious localization of damage and nonphysical dependence on mesh resolution. Finally, a more sophisticated scheme for advecting damage is needed [e.g., *Albrecht and Levermann*, 2014] to prevent artifical diffusion and maintain sharp gradients in flow caused by fractures.

3.5. Diagnostic Capability of New Framework

This new framework can be used as a diagnostic tool to assess the susceptibility to weakening of any ice shelf, from a single time period of observations. For example, in 2000 RLBIS had relatively stable levels of damage; much of the ice shelf could sustain some increase in strain rate before damage would have to increase (Figure 2b). In the same manner, the "criticality" of damage for other ice shelves can now be assessed according to the proximity of their parameter spaces to the envelope curve for damage. This assumes that the parameters τ_o and κ determined here are applicable for other ice shelves, an assumption that can only be tested once similar observational time series become available for ice shelves also undergoing significant mechanical change. However, since RLBIS has undergone a substantial perturbation (partial ice shelf collapse) and subsequent progressive weakening over the assembled time series, this ice shelf is ideal for developing such a generalized constitutive framework. It is more likely than any other to have fully swept out the possible constitutive parameter space for viscous deformation and damage. Thus, it is reasonable to suggest that the parameter values determined here should be applicable in other places and contexts.

4. Conclusions

Ice shelf buttressing is clearly linked to some of the largest recent changes to the Antarctic ice sheet. Mechanical weakening of ice shelves may accelerate buttressing losses and associated ice sheet discharge beyond what has been predicted by ice sheet models to date. Based on the observed degradation of the remnant Larsen B Ice Shelf, a new generalized constitutive framework for viscous ice deformation and weakening was developed. Most of the observed weakening of the ice shelf through time, especially in critical shear margins, is consistent with this approach to viscous damage formation and growth.

The promise of this new framework is thus in its general applicability, both for diagnosing the state of health of existing ice shelves and for predicting their degradation and demise as they are threatened by melting from above and below. This new framework is not specific to this particular ice shelf or even to ice shelves, in general. The framework can serve as a foundation for modeling other glaciological processes involving fracture-induced enhancement of viscous ice deformation. Processes such as marginal weakening of ice streams, crevasse formation and growth, and meltwater routing and hydrofracture can all be modeled using this framework. The improved physical representation of processes related to fracturing and weakening of ice will lead to better model projections of ice sheet evolution and sea level rise in a warming climate.

Acknowledgments

This work was performed at the University Centre in Svalbard, the University of California, Irvine, and the Jet Propulsion Laboratory-California Institute of Technology, under a contract with NASA. A.K., B.S., E.L., E.R., and M.M. were supported by grants from NASA's Cryospheric Sciences Program. SAR data acquisitions were coordinated through the Polar Space Task Group. The source code for the model used in this study, the Ice Sheet System Model (ISSM), is freely available via issm.jpl.nasa.gov. The input files and data necessary to reproduce the results using ISSM are available from the authors upon request (chris.borstad@unis.no).

References

Albrecht, T., and A. Levermann (2014), Fracture-induced softening for large-scale ice dynamics, *Cryosphere*, *8*(2), 587–605, doi:10.5194/tc-8-587-2014.

Bassis, J., R. Coleman, H. Fricker, and J. Minster (2005), Episodic propagation of a rift on the Amery Ice Shelf, East Antarctica, *Geophys. Res. Lett.*, *32*, L06502, doi:10.1029/2004GL022048.

Bažant, Z. P., and M. Jirásek (2002), Nonlocal integral formulations of plasticity and damage: Survey of progress, *J. Eng. Mech.*, *128*(11), 1119–1149, doi:10.1061/(ASCE)0733-9399(2002)128:11(1119).

Borstad, C. P., and D. M. McClung (2011), Numerical modeling of tensile fracture initiation and propagation in snow slabs using nonlocal damage mechanics, *Cold Reg. Sci. Technol.*, *69*, 145–155, doi:10.1016/j.coldregions.2011.09.010.

Borstad, C. P., A. Khazendar, E. Larour, M. Morlighem, E. Rignot, M. P. Schodlok, and H. Seroussi (2012), A damage mechanics assessment of the Larsen B Ice Shelf prior to collapse: Toward a physically-based calving law, *Geophys. Res. Lett.*, *39*, L18502, doi:10.1029/2012GL053317.

Borstad, C. P., E. Rignot, J. Mouginot, and M. P. Schodlok (2013), Creep deformation and buttressing capacity of damaged ice shelves: Theory and application to Larsen C Ice Shelf, *Cryosphere*, *7*, 1931–1947, doi:10.5194/tc-7-1931-2013.

Cuffey, K., and W. S. B. Paterson (2010), *The Physics of Glaciers*, 4th ed., Elsevier, Oxford, U. K.

Duddu, R., and H. Waisman (2012), A temperature dependent creep damage model for polycrystalline ice, *Mech. Mater.*, *46*, 23–41, doi:10.1016/j.mechmat.2011.11.007.
Fretwell, P., et al. (2013), Bedmap2: Improved ice bed, surface and thickness datasets for Antarctica, *Cryosphere*, *7*(1), 375–393.
Fricker, H. A., and L. Padman (2012), Thirty years of elevation change on Antarctic Peninsula ice shelves from multimission satellite radar altimetry, *J. Geophys. Res.*, *117*, C02026, doi:10.1029/2011JC007126.
Goldberg, D. N., C. M. Little, O. V. Sergienko, A. Gnanadesikan, R. Hallberg, and M. Oppenheimer (2012), Investigation of land ice-ocean interaction with a fully coupled ice-ocean model: 1. Model description and behavior, *J. Geophys. Res.*, *117*, F02037, doi:10.1029/2011JF002246.
Gudmundsson, G. H. (2013), Ice-shelf buttressing and the stability of marine ice sheets, *Cryosphere*, *7*(2), 647–655, doi:10.5194/tc-7-647-2013.
Hellmer, H. H., F. Kauker, R. Timmermann, J. Determann, and J. Rae (2012), Twenty-first-century warming of a large Antarctic ice-shelf cavity by a redirected coastal current, *Nature*, *485*(7397), 225–228, doi:10.1038/nature11064.
Holland, D., and A. Jenkins (1999), Modeling thermodynamic ice-ocean interactions at the base of an ice shelf, *J. Phys. Oceanogr.*, *29*, 1787–1800.
Intergovernmental Panel on Climate Change (2013), *Climate Change 2013: The Physical Science Basis. Contribution of Working Group I to the Fifth Assessment Report of the Intergovernmental Panel on Climate Change*, Cambridge Univ. Press, Cambridge, U. K.
Joughin, I., B. Smith, and B. Medley (2014), Marine ice sheet collapse potentially underway for the Thwaites glacier basin, West Antarctica, *Science*, *344*(6185), 735–738, doi:10.1126/science.1249055.
Khazendar, A., E. Rignot, and E. Larour (2011), Acceleration and spatial rheology of Larsen C Ice Shelf, Antarctic Peninsula, *Geophys. Res. Lett.*, *38*, L09502, doi:10.1029/2011GL046775.
Khazendar, A., C. P. Borstad, B. Scheuchl, E. Rignot, and H. Seroussi (2015), The evolving instability of the remnant Larsen B Ice Shelf and its tributary glaciers, *Earth Planet. Sci. Lett.*, *419*, 199–210, doi:10.1016/j.epsl.2015.03.014.
Krug, J., J. Weiss, O. Gagliardini, and G. Durand (2014), Combining damage and fracture mechanics to model calving, *Cryosphere*, *8*(6), 2101–2117, doi:10.5194/tc-8-2101-2014.
Larour, E., E. Rignot, I. Joughin, and D. Aubry (2005), Rheology of the Ronne Ice Shelf, Antarctica, inferred from satellite radar interferometry data using an inverse control method, *Geophys. Res. Lett.*, *32*, L05503, doi:10.1029/2004GL021693.
Larour, E., H. Seroussi, M. Morlighem, and E. Rignot (2012), Continental scale, high order, high spatial resolution, ice sheet modeling using the Ice Sheet System Model (ISSM), *J. Geophys. Res.*, *117*, F01022, doi:10.1029/2011JF002140.
MacAyeal, D. (1989), Large-scale ice flow over a viscous basal sediment: Theory and application to Ice Stream B, Antarctica, *J. Geophys. Res.*, *94*(B4), 4071–4087.
MacGregor, J. A., G. A. Catania, M. S. Markowski, and A. G. Andrews (2012), Widespread rifting and retreat of ice-shelf margins in the eastern Amundsen Sea Embayment between 1972 and 2011, *J. Glaciol.*, *58*(209), 458–466.
Morlighem, M., H. Seroussi, E. Larour, and E. Rignot (2013), Inversion of basal friction in Antarctica using exact and incomplete adjoints of a higher-order model, *J. Geophys. Res. Earth Surf.*, *118*, 1746–1753, doi:10.1002/jgrf.20125.
Pralong, A., and M. Funk (2005), Dynamic damage model of crevasse opening and application to glacier calving, *J. Geophys. Res.*, *110*, B01309, doi:10.1029/2004JB003104.
Pritchard, H. D., S. R. M. Ligtenberg, H. A. Fricker, D. G. Vaughan, M. R. van den Broeke, and L. Padman (2012), Antarctic ice-sheet loss driven by basal melting of ice shelves, *Nature*, *484*(7395), 502–505, doi:10.1038/nature10968.
Rignot, E., J. Mouginot, and B. Scheuchl (2011), Antarctic grounding line mapping from differential satellite radar interferometry, *Geophys. Res. Lett.*, *38*, L10504, doi:10.1029/2011GL047109.
Rignot, E., S. Jacobs, J. Mouginot, and B. Scheuchl (2013), Ice shelf melting around Antarctica, *Science*, *341*(6143), 266–270, doi:10.1126/science.1235798.
Rignot, E., J. Mouginot, M. Morlighem, H. Seroussi, and B. Scheuchl (2014), Widespread, rapid grounding line retreat of Pine Island, Thwaites, Smith and Kohler glaciers, West Antarctica from 1992 to 2011, *Geophys. Res. Lett.*, *41*, 3502–3509, doi:10.1002/2014GL060140.
Scambos, T. A., E. Berthier, T. Haran, C. A. Shuman, A. J. Cook, S. R. M. Ligtenberg, and J. Bohlander (2014), Detailed ice loss pattern in the northern Antarctic Peninsula: Widespread decline driven by ice front retreats, *Cryosphere*, *8*(6), 2135–2145, doi:10.5194/tc-8-2135-2014.
Shepherd, A., D. Wingham, T. Payne, and P. Skvarca (2003), Larsen Ice Shelf has progressively thinned, *Science*, *302*(5646), 856–859.
Sinha, N. K. (1988), Crack-enhanced creep in polycrystalline material: Strain-rate sensitive strength and deformation of ice, *J. Mater. Sci.*, *23*(12), 4415–4428, doi:10.1007/BF00551940.
van den Broeke, M. R., and N. P. van Lipzig (2004), Changes in Antarctic temperature, wind and precipitation in response to the Antarctic Oscillation, *Ann. Glaciol.*, *39*(1), 119–126.